The Abdus Salam International Centre for Theoretical Physics

United Nations Educational, Scientific and Cultural Organization

IAEA International Atomic Energy Agency

CENTRAL EUROPEAN INITIATIVE

2265-7

Advanced School on Understanding and Prediction of Earthquakes and other Extreme Events in Complex Systems

26 September - 8 October, 2011

EARTHQUAKE PREDICTION AND PREVENTION FOR A DISASTER RESILIENT SOCIETY

G.F. Panza

University of Trieste/SAND Group ICTP
Trieste

EARTHQUAKE PREDICTION AND PREVENTION FOR A DISASTER RESILIENT SOCIETY

G.F. Panza and the SAND group

Advanced School on Understanding and Prediction of Earthquakes and other Extreme Events in Complex Systems

Trieste, September 26 – October 8, 2011

INTRODUCTION

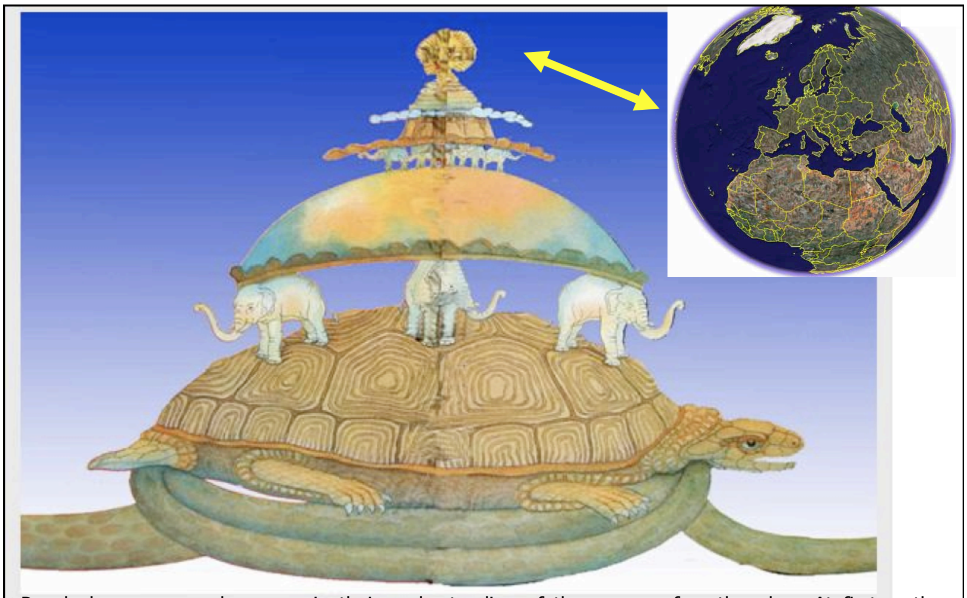

People have come a long way in their understanding of the causes of earthquakes. At first myths, legends, and apocalyptic imaginations were used to explain processes in the Earth's interior. Prior to the knowledge that the Earth is a sphere, the Earth was thought to be a disk carried by something. **Hindu mythology** taught that the god Vishnu, **preserver of the world,** is lying on the world snake. On the turtle stand **four** elephants that carry the Earth. **Movement of the elephants causes earthquakes.**

3

Progresses in the mitigation of hazard can rely upon the control of the dance of the elephants!???

Certainly not !!

Seismic risk can be reduced only with the joint exploitation of advanced seismic engineering techniques and reliable methodologies for the assessment of seismic hazard.

4

In **1660** *Robert Hooke* formulates de fundamental law of elasticity

Ut tensio sic vis

the base of the Physics of Seismology

5

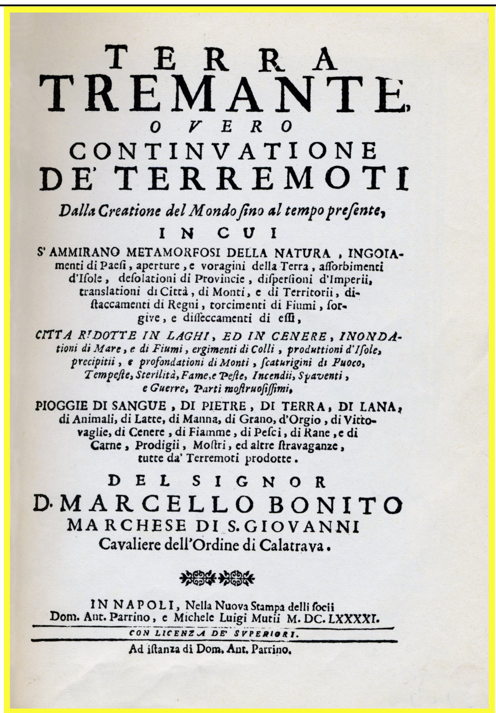
TERRA
TREMANTE,
OVERO
CONTINVATIONE
DE' TERREMOTI
Dalla Creatione del Mondo sino al tempo presente,
IN CUI
S'AMMIRANO METAMORFOSI DELLA NATURA, INGOIAmenti di Paesi, aperture, e voragini della Terra, assorbimenti d'Isole, desolationi di Provincie, dispersioni d'Imperii, translationi di Città, di Monti, e di Territorii, distaccamenti di Regni, torcimenti di Fiumi, sorgive, e disseccamenti di essi,
CITTA RIDOTTE IN LAGHI, ED IN CENERE, INONDAtioni di Mare, e di Fiumi, ergimenti di Colli, produttioni d'Isole, precipitii, e profondationi di Monti, scaturigini di Fuoco, Tempeste, Sterilità, Fame, e Peste, Incendii, Spaventi, e Guerre, Parti mostruosissimi,
PIOGGIE DI SANGUE, DI PIETRE, DI TERRA, DI LANA, di Animali, di Latte, di Manna, di Grano, d'Orgio, di Vittovaglie, di Cenere, di Fiamme, di Pesci, di Rane, e di Carne, Prodigii, Mostri, ed altre stravaganze, tutte da' Terremoti prodotte.
DEL SIGNOR
D. MARCELLO BONITO
MARCHESE DI S. GIOVANNI
Cavaliere dell'Ordine di Calatrava.
IN NAPOLI, Nella Nuova Stampa delli socii Dom. Ant. Parrino, e Michele Luigi Mutii M. DC. LXXXXI.
CON LICENZA DE' SVPERIORI.
Ad istanza di Dom. Ant. Parrino.

In 1691 the Author describes the effects of the catastrophic earthquake that December 5, 1456 shook L'Aquila and neighbors and produced severe damages to a region very similar to the one affected by the catastrophic event of April 6, 2009.

6

Only in 1760, the scientific community, thanks to the work of John Michell, recognized that earthquakes and volcanic eruptions are endogenous natural phenomena of the Earth.

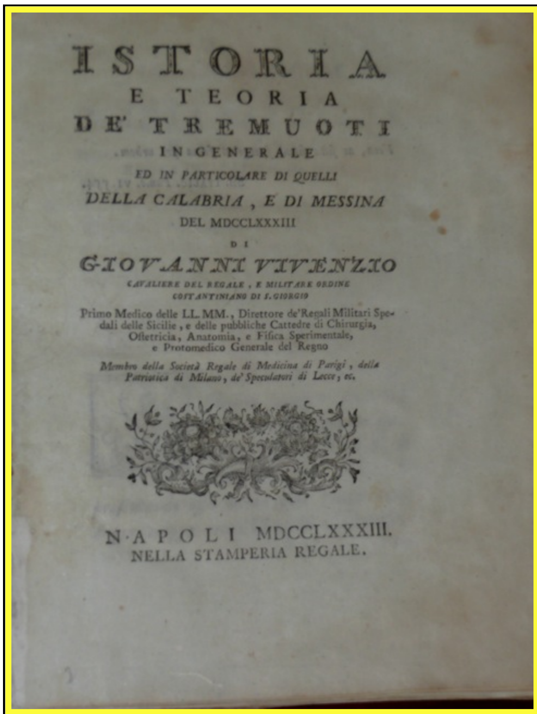
ISTORIA
E TEORIA
DE' TREMUOTI
IN GENERALE
ED IN PARTICOLARE DI QUELLI
DELLA CALABRIA, E DI MESSINA
DEL MDCCLXXXIII
DI
GIOVANNI VIVENZIO
CAVALIERE DEL REGALE, E MILITARE ORDINE
COSTANTINIANO DI S. GIORGIO
Primo Medico delle LL. MM., Direttore de' Regali Militari Spedali delle Sicilie, e delle pubbliche Cattedre di Chirurgia, Ostetricia, Anatomia, e Fisica Sperimentale, e Protomedico Generale del Regno
Membro della Società Regale di Medicina di Parigi, della Patriotica di Milano, de' Speculatori di Lecce, ec.
NAPOLI MDCCLXXXIII.
NELLA STAMPERIA REGALE.

In the late 1700, stimulated by the study on electricity, electroseismic theories are formulated and in analogy with Benjamin Franklin (lightning rod), Pierre Bertholon conceives the idea of an "earthquake rod" (Journal de physique, 1779). Giovanni Vivenzio in his book "Historia e Teoria de tremuoti in generale ed in particolare di quelli della Calabria e di Messina del 1783", published the same year, says that: "...i tremuoti non sono altro che tuoni sotterranei siccome Plinio l' ha conosciuto anticamente; e poiché è dimostrato che il tuono è effetto di elettricità, non si può far di meno di riconoscere la materia elettrica per cagione dei tremuoti".

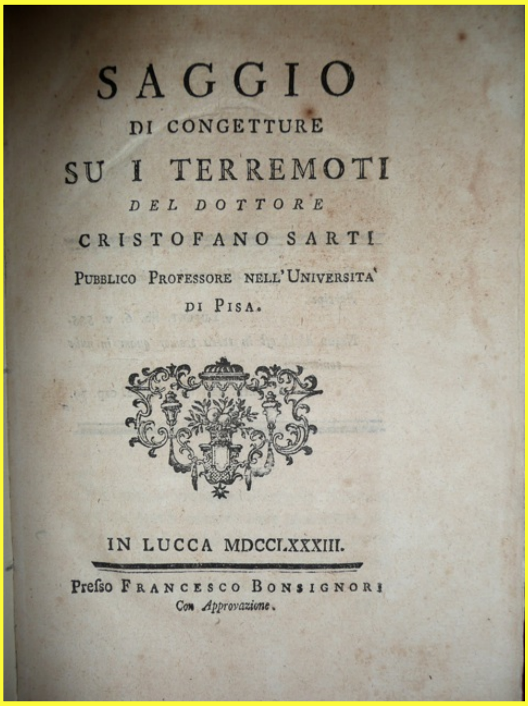

SAGGIO
DI CONGETTURE
SU I TERREMOTI
DEL DOTTORE
CRISTOFANO SARTI
PUBBLICO PROFESSORE NELL'UNIVERSITA'
DI PISA.

IN LUCCA MDCCLXXXIII.
Presso FRANCESCO BONSIGNORI
Con Approvazione.

Cristofano Sarti, in his book, published in 1788 works out a series of conjectures about the endogenous origin of the earthquake and he has the great merit to point out that earthquakes and volcanoes are natural phenomena not necessarily correlated.

9

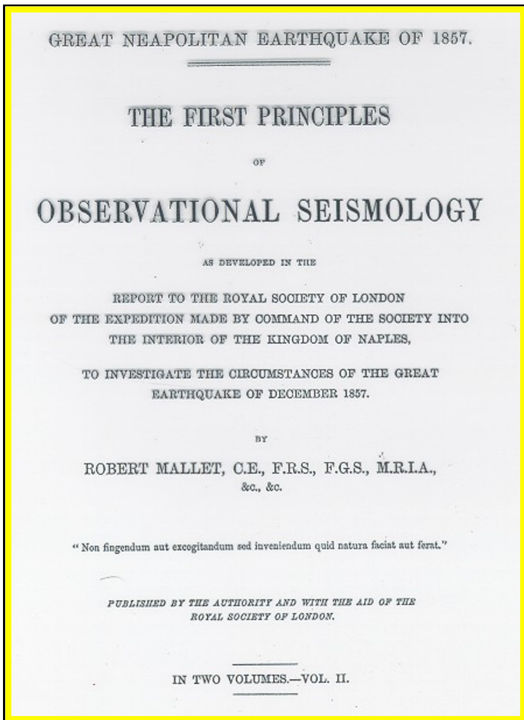

GREAT NEAPOLITAN EARTHQUAKE OF 1857.

THE FIRST PRINCIPLES
OF
OBSERVATIONAL SEISMOLOGY
AS DEVELOPED IN THE
REPORT TO THE ROYAL SOCIETY OF LONDON
OF THE EXPEDITION MADE BY COMMAND OF THE SOCIETY INTO
THE INTERIOR OF THE KINGDOM OF NAPLES,
TO INVESTIGATE THE CIRCUMSTANCES OF THE GREAT
EARTHQUAKE OF DECEMBER 1857.

BY
ROBERT MALLET, C.E., F.R.S., F.G.S., M.R.I.A.,
&c., &c.

"Non fingendum aut excogitandum sed inveniendum quid natura faciat aut ferat."

PUBLISHED BY THE AUTHORITY AND WITH THE AID OF THE ROYAL SOCIETY OF LONDON.

IN TWO VOLUMES.—VOL. II.

The Irish engineer Robert Mallet, with a grant of 150 pounds from the Royal Society of London, invited by Francesco II di Borbone, made a scientific survey of the most damaged area by the 1857 earthquake, that hit South Italy. Mallet collected all his observations in a monumental publication (1862) the Royal Society of London that represents the first attempt to apply systematically the basic principles of Physics to the effects of earthquakes.

1902 *Giuseppe Mercalli* publishes the macrosesimic Intensity scale.

1907 *Vito Volterra* publishes the theory of dislocation, based on Somigliana solution of Navier equations and he opens the way to the study of the Physics of seismic sources.

11

Italy is the forefront of seismological research and seismic hazard mitigation till the beginning of 1900. There is a severe and guilty decline, mostly due to governmental deficiencies, that is reversed, for the first time, after the 1976 Friuli earthquake. This constructive trend seems to continue in 2003 after the San Giuliano di Puglia earthquake of 2002 and after the 2009 l'Aquila earthquake. The activity of ICTP started in the 80s, in collaboration with MITPAN-Moscow scientists, is certainly a part of this Renaissance, with a special attention to prevention.

12

Building a culture of prevention is not easy. While the costs of prevention have to be paid in the present, its benefits lie in a distant future. Moreover, the benefits are not tangible; they are the disasters that did NOT happen.

- Kofi Annan,1999

The evaluation of seismic hazard is often based on the traditional Probabilistic Seismic Hazard Analysis, i.e. on the probabilistic analysis of earthquake catalogues and of ground motion, from macroseismic observations and instrumental recordings. This leads to severe bias in the estimation of seismic hazard, because the mathematical model of PSHA, as it is in use today, is inaccurate and leads to systematic errors in the calculation process.

14

This approach has been proven unreliable in providing seismic hazard assessment by many events occurred in the recent past, possibly due to the insufficient information about historical seismicity, which can introduce relevant errors in the purely statistical approach mainly based on the seismic history.

15

? GSHAP ?
Checking forecasted values against observations

The probabilistic analysis supplies indications that can be useful but not sufficiently reliable to characterize seismic hazard.

Lessons from recent earthquakes: Kobe (17.1.1995), Gujarat (26.1.2001), Boumerdes (21.5.2003), Bam (26.12.2003) and Eastern Sichuan (12.5.2008), Haiti (12.1.2010)

	PGA(g) Expected with a probability of exceedence of 10% in 50 years (return period 475 years)	Observed
Kobe	0.40-0.48	0.7-0.8
Gujarat	0.16-0.24	0.5-0.6
Boumerdes	0.08-0.1	0.3-0.4
Bam	0.16-0.24	0.7-0.8
E-Sichuan	0.16-0.24	0.6->0.8
Haiti	0.08-0.16	0.35-0.4

MORE LESSONS in 2011

Location	Date	Magnitude	Intensity difference	Casualties
Sendai (Japan)	11.03.2011	9.0	3.3 (III)	> 20.000 ??
Port-au-Prince (Haiti)	12.01.2010	7.3	2.2 (II)	222.570
Padang (Southern Sumatra, Indonesia)	30.09.2009	7.5	1.8 (II)	1.117
Wenchuan (Sichuan, China)	12.05.2008	8.1	3.2 (III)	87.587
Yogyakarta (Java, Indonesia)	26.05.2006	6.3	0.3 (0)	5.749
Kashmir (North India and Pakistan border region)	08.10.2005	7.7	2.3 (II)	86.000
Nias (Sumatra, Indonesia)	28.03.2005	8.6	3.3 (III)	1.313
Sumatra-Andaman (Indian Ocean)	26.12.2004	9.0	4.0 (IV)	227.898
Bam (Iran)	26.12.2003	6.6	0.2 (0)	31.000
Boumerdes (Algeria)	21.05.2003	6.8	2.1 (II)	2.266
Bhuj (Gujarat, India)	26.01.2001	8.0	2.9 (III)	20.085

List of the Top Eleven deadliest earthquakes occurred during the period 2000-2011, and the corresponding intensity differences, $DI_0 = I_0(M) - I_0(mPGA)$, among the observed values and predicted by GSHAP. $I_0(M)$ and $I_0(mPGA)$ are computed from the observed magnitude M and the maximum GSHAP PGA around the observed epicentre, respectively, using existing relationships (after Kossobokov and Nekrasova (2010)).

If we include in the list the 1995 Kobe event, we see that Japan has been hit by two surprises in the last 25 years!!

Earthquake	Date	Latitude	Longitude	Depth, km	USGS Magnitude	GSHAP PGA, m/s^2	GSHAP Magnitude	dM
Bhuj, India	2001/01/26	23.42°N	70.23°E	16	8.0	2.050	6.1	1.9
Boumerdes, Algeria	2003/05/21	36.96°N	3.63°E	10	6.9	0.729	5.2	1.7
Bam, Iran	2003/12/26	29.10°N	58.35°E	4	6.8	3.780	6.6	0.2
Nias, Sumatra	2005/03/28	2.09°N	97.11°E	25	8.6	2.897	6.4	2.2
Kashmir, Pakistan	2005/10/08	34.54°N	73.59°E	10	7.7	2.111	6.1	1.6
Yogyakarta, Indonesia	2006/05/26	7.96°S	110.45°E	16	6.3	2.030	6.1	0.2
Wenchuan, China	2008/05/12	31.00°N	103.32°E	10	8.1	1.686	5.9	2.2
Padang, Sumatra	2009/09/30	0.72°S	99.87°E	81	7.6	2.580	6.3	1.3
Haiti	2010/01/12	18.44°N	72.57°W	10	7.0	1.456	5.8	1.5
Qinghai, China	2010/04/13	33.22°N	96.67°E	17	7.0	1.112	5.6	1.4
Sumatra-Andaman	2004/12/26	3.30°N	95.98°E	30	9.1	2.768	6.4	2.7
Tōhoku, Japan	2011/03/11	38.30°N	142.37°E	32	9.0	4.895	6.8	2.2

Table 1: Source parameters (http://earthquake.usgs.gov/earthquakes/eqinthenews/) of the earthquakes studied. Columns seven and eight list the largest peak ground accelerations given by GSHAP within a box 11 km on a side around the epicenter of the disastrous earthquakes, and the magnitude of an earthquake at that location, which would generate the PGA given by GSHAP, respectively. dM is the difference between the magnitude observed and the magnitude implied by the GSHAP map.

Wyss et al., 2011

Earthquake	Fatalities				Settlements affected			Population affected		
	observed	estimate	GSHAP	Ratio	estimate	GSHAP	Ratio	estimate	GSHAP	Ratio
Bhuj, India	20,000	19,500	300	65	2,930	880	3	84,991,000	1,328,000	64
Boumerdes, Algeria	2,300	2,200	1	2200	1,350	330	4	11,197,000	1,855,000	6
Bam, Iran	30,000	13,500*	11,500*	1	8,990	6,790	1	1,676,000	951,000	2
Nias, Sumatra	1,600	1,800	1	1800	3,880	370	10	13,291,000	6,000	2,215
Kashmir, Pakistan	86,000	71,600#	3,800#	19	9,040	3,170	3	63,726,000	4,723,000	13
Yogyakarta, Indonesia	5,700	6,200	3,000	2	12,170	220	55	19,100,000	16,338,000	1
Wenchuan, China	87,000	86,800#	500#	174	4,560	1,270	4	57,230,000	8,544,000	7
Padang, Sumatra	1,100	1,100	1	1100	3,070	1,020	3	10,859,000	563,830	19
Haiti	100,000	98,500#	5,800#	17	9,620	6,860	1	10,449,000	5,271,000	2
Qinghai, China	3,000	2,700*	20*	135	1,390	220	6	2,405,000	543,000	4
Sumatra-Andaman	NA	9,800	1	9800	3,330	1	3,330	10,416,000	1	$>10^7$
Tōhoku, Japan	NA	3,200	1	3200	1,030	50	21	59,913,000	2,804,000	21

Table 2: Comparison of observed numbers of fatalities with those calculated by QLARM for the reported magnitude (estimate) and the magnitude implied by GSHAP. The columns entitled "Settlements affected" and "Population affected" list the respective numbers for settlements with at least slight damage (blue to black dots in Fig. 1) calculated for the observed magnitude (estimate) and the magnitude implied by GSHAP.

Tohoku estimated fatalities about 20000

Wyss et al., 2011

To overcome the mentioned limitations and, above all, to improve the pre-seismic information which may lead to an effective mitigation of seismic risk, we are following an innovative approach, that combines Earth Observation (EO) data and new advanced approaches in seismological and geophysical data analysis.

20

ASI Pilot Project - SISMA

"Seismic Information System for Monitoring and Alert"

R. Sabadini[(1)], R. Barzaghi[(2)], G.F. Panza[(3,6)], M. Fermi[(4)], B. Crippa[(1)], A. Peresan[(3)], F. Vaccari[(3)], A. Aoudia[(6)], F. Romanelli[(3)], R. Riva[(1)], A. M. Marotta [(1)], S. Zoffoli[(5)] and R. Guzzi[(5)]

(1) Dipartimento di Scienze della Terra, Università di Milano, Italy
(2) Dipartimento di Scienze della Terra, Università di Trieste, Italy
(3) Politecnico di Milano, Italy
(4) Galileian Plus, Italy
(5) Agenzia Spaziale Italiana, Sezione Osservazione della Terra
(6) The Abdus Salam International Centre for Theoretical Physics. Trieste, Italy

agenzia spaziale italiana | DST | Università di Milano | Politecnico di Milano | galileian PLUS

21

The system we are developing is based on the neodeterministic approach for the estimation of seismic ground motion, integrated with the space and time dependent information provided by EO data analysis through geophysical forward modeling.

22

The need of integration of different geophysical observables is obvious when the process of earthquake preparation and occurrence is analysed: the lithosphere - a hierarchical system of interacting blocks - accumulates stress, according to strain and strain rates fields due to tectonics, which is partly released during the earthquake occurrence.

23

System's Overall Description

24

Seismological data analysis

- INPUT

Data on seismicity (earthquake catalogues), geomorphology and geodynamics and Earth structure (velocity, gravity data);

Worldwide tested pattern recognition algorithms for middle-range intermediate-term earthquake prediction and for identification of areas prone to damaging earthquakes;

Robust and tested codes for the Earth structure retrieval and numerical modelling of lithosphere block dynamics.

Seismological data analysis

- **OUTPUT (1)**

Regional alerted areas by the near real time monitoring of seismicity (TIPs for the occurrence of earthquakes with $M \geq M_0$);

Maps of the morphostructural zonation and selection of seismogenic nodes prone to earthquakes with M≥6.0 & M≥6.5 within the alerted regions;

Seismological data analysis

- **OUTPUT (2)**

Restrained local alerted areas for GPS and SAR investigations;

Multiscale velocity models of the Earth structure for geophysical forward modelling;

Preferred models for the dynamics of the lithosphere at a regional scale.

Real-time monitoring of the seismic flow: CN and M8S algorithms

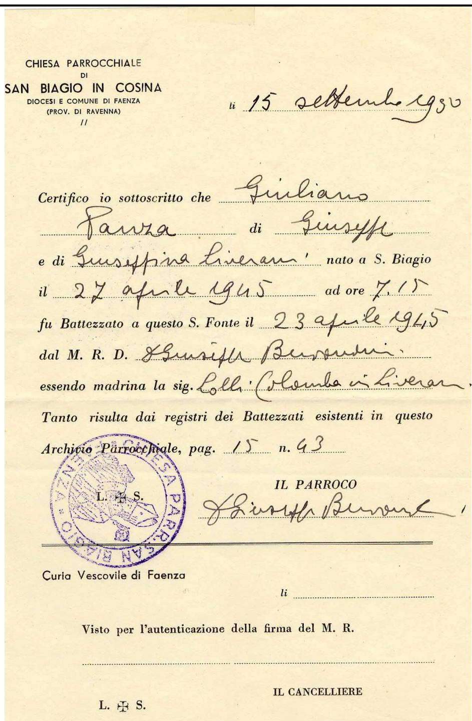

CHIESA PARROCCHIALE
DI
SAN BIAGIO IN COSINA
DIOCESI E COMUNE DI FAENZA
(PROV. DI RAVENNA)

li 15 settembre 1950

Certifico io sottoscritto che Giuliano Panza di Giuseppe e di Giuseppina Liverani nato a S. Biagio il 27 aprile 1945 ad ore 7.15 fu Battezzato a questo S. Fonte il 23 aprile 1945 dal M. R. D. Giuseppe Bernardini essendo madrina la sig. Lelli Colomba in Liverani.

Tanto risulta dai registri dei Battezzati esistenti in questo Archivio Parrocchiale, pag. 15 n. 43

L. ✠ S.

IL PARROCO
Giuseppe Bernardini

Curia Vescovile di Faenza

li ....

Visto per l'autenticazione della firma del M. R.

L. ✠ S.

IL CANCELLIERE

My earliest credential about prediction

This is my certificate of baptism, drafted on September 15, 1950, stating that I was **born** on April **27**, 1945 and I was **christened** on April **23**,1945

29

Intermediate-term middle-range earthquake prediction experiment

CN algorithm (*Keilis-Borok et al., 1990; Peresan et al., 2005*)
M8S algorithm (*Kossobokov et al, 2002)*

Main features:

- **Fully formalized algorithms and computer codes available for independent testing;**
- **Use of published & routine catalogues of earthquakes;**
- **Worldwide tests ongoing for more than 10 years permitted to assess the significance of the issued predictions** (*Kossobokov et al., 1999; Rotwain and Novikova, 1999)*

Intermediate-term middle-range earthquake prediction experiment in Italy

CN and M8S algorithms are based on a set of empirical functions of time to allow for a quantitative analysis of the premonitory patterns which can be detected in the seismic flow:

- **Variations in the seismic activity**
- **Seismic quiescence**
- **Space-time clustering of events**

They allow to identify the TIPs
(Times of Increased Probability)
for the occurrence of a strong earthquake within a delimited region

Intermediate-term middle-range earthquake prediction experiment in Italy

- **Stability tests with respect to several free parameters of the algorithms** *(e.g. Costa et al., 1995; Peresan et al., GJI, 2000; Peresan et al., PEPI, 130, 2002);*
- **CN predictions are regularly updated every two months since January 1998;**
- **M8S predictions are regularly updated every six months since January 2002;**

Real time prediction experiment started in July 2003

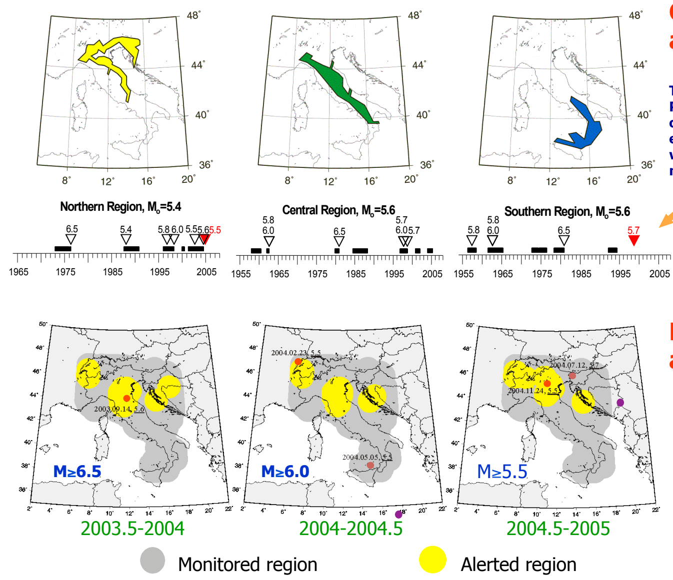

CN algorithm

Times of Increased Probability for the occurrence of events with M>Mo within the monitored regions

M8s algorithm

Events with $M_{max} \geq 5.5$ occurred since July 2003

Updated to January 2007

Intermediate-term middle-range earthquake prediction in Italy

Prediction experiment: launched starting on July 2003, is aimed at a *real-time test* of CN and M8S predictions in Italy. Updated predictions are regularly posted at:

"http://www.ictp.trieste.it/www_users/sand/prediction/prediction.htm"

A complete archive of predictions is made accessible to a number of scientists, with the goal to accumulate a collection of correct and wrong predictions, that will permit to validate the considered methodology.

Current predictions are protected by password. Although these predictions are intermediate-term and by no means imply a "red alert", there is a legitimate concern about maintaining necessary confidentiality.

Intermediate-term middle-range earthquake prediction

Space-time volume of alarm in M8S application in Italy

Experiment	M6.5+		M6.0+		M5.5+	
	Space-time volume, %	n/N	Space-time volume, %	n/N	Space-time volume, %	n/N
Retrospective (1972-2001)	36	2/2	40	1/2	39	9/14
Forward (2002-2009)	35	0/0	39	0/1	20	5/9
All together (1972-2009)	36	2/2	40	1/3	35	14/23

Algorithm M8s predicted 60% of the events occurred in the monitored zones in Italy, i.e. 17 out of 28 events occurred within the area alerted for the corresponding magnitude range. The confidence level of M5.5+ predictions since 1972 has been estimated to be above 98%; no estimation is yet possible for other magnitude levels.

(updated to July 1 2009; next updating January 1 2010)

A complete archive of M8S predictions in Italy can be viewed at:
http://www.ictp.trieste.it/www_users/sand/prediction/prediction.htm
http://www.mitp.ru/prediction.htm

e-mail: lina@mitp.ru

Intermediate-term middle-range earthquake prediction

Space-time volume of alarm in CN application in Italy

Experiment	Space-time volume of alarm (%)	n/N	Confidence level (%)
Retrospective* (1954 – 1963)	41	3/3	93
Retrospective (1964 – 1997)	27	5/5	>99
Forward (1998 – 2009)	27	4/6	95
All together (1954 – 2009)	29	12/14	>99

* Central and Southern regions only

Algorithm CN predicted 12 out of the 14 strong earthquakes occurred in the monitored zones of Italy, with less than 30% of the considered space-time volume occupied by alarms.

(updated to September 1 2009; next updating November 1 2009)

A complete archive of CN predictions in Italy can be viewed at:
http://www.ictp.trieste.it/www_users/sand/prediction/prediction.htm

e-mail: aperesan@units.it

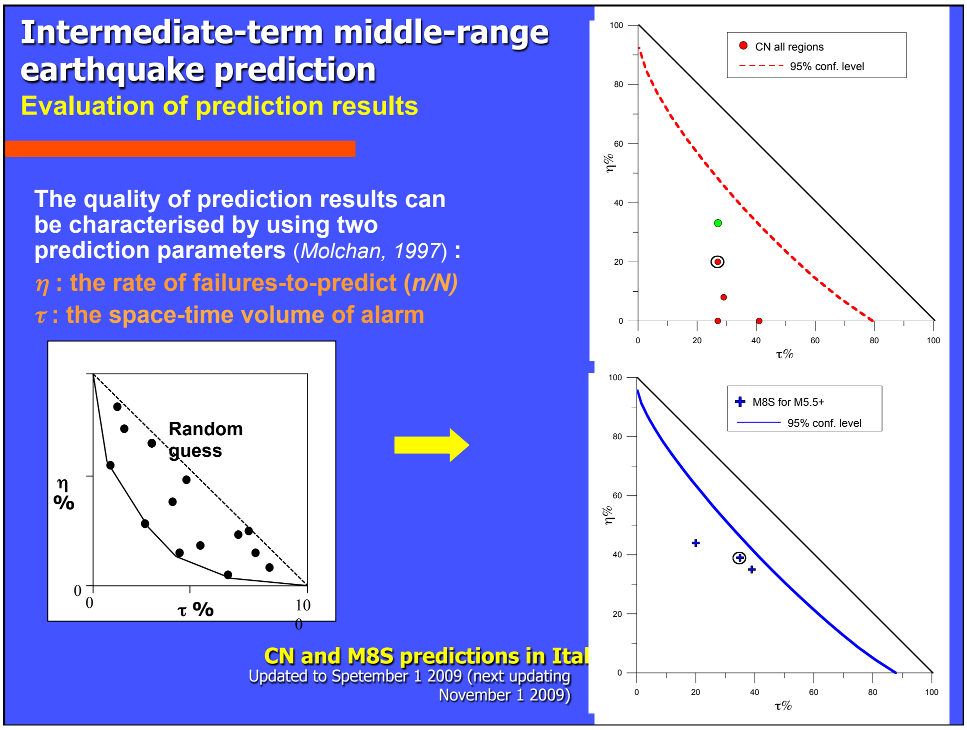
Intermediate-term middle-range earthquake prediction
Evaluation of prediction results
The quality of prediction results can be characterised by using two prediction parameters (Molchan, 1997) :
η : the rate of failures-to-predict (n/N)
τ : the space-time volume of alarm
Random guess
η %
τ %
CN and M8S predictions in Ital
Updated to Spetember 1 2009 (next updating November 1 2009)
CN all regions
95% conf. level
M8S for M5.5+
95% conf. level
η%
τ%

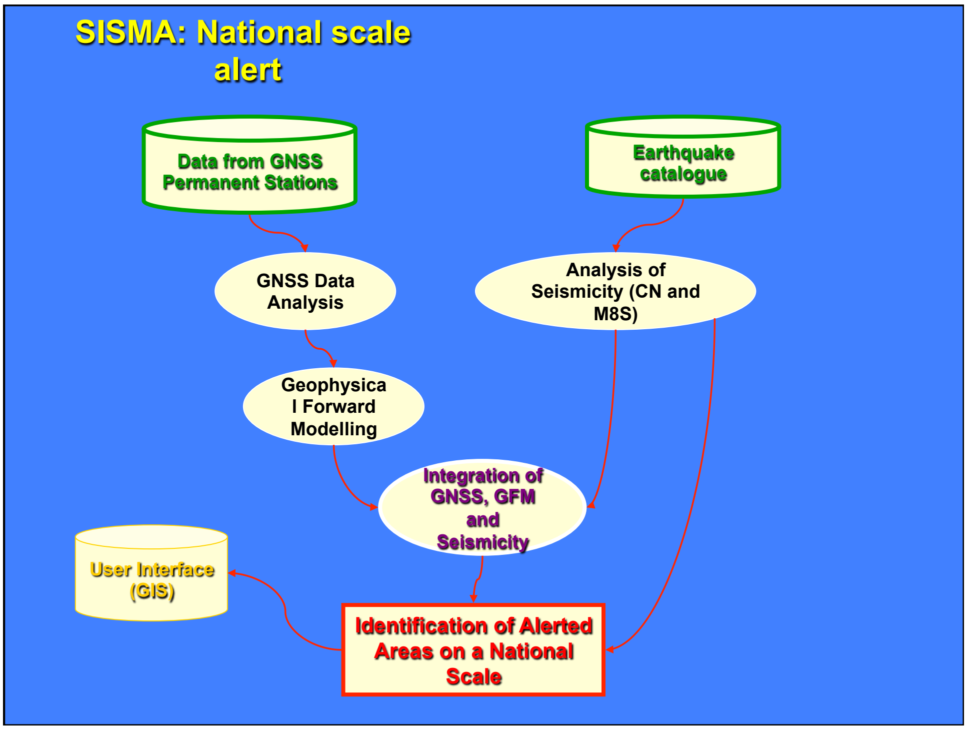
SISMA: National scale alert
Data from GNSS Permanent Stations
Earthquake catalogue
GNSS Data Analysis
Analysis of Seismicity (CN and M8S)
Geophysical Forward Modelling
Integration of GNSS, GFM and Seismicity
User Interface (GIS)
Identification of Alerted Areas on a National Scale

Alerted Areas at National scale

Integrating information from GNSS anomalies identified at national scale
and alerted areas identified by the pattern recognition analysis of seismicity

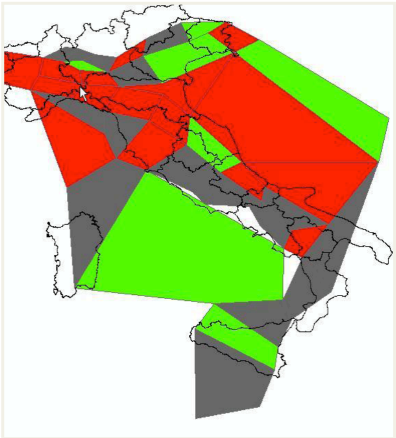

Map of GNSS anomalies
(red: anomaly; green: no anomaly; gray: no data)

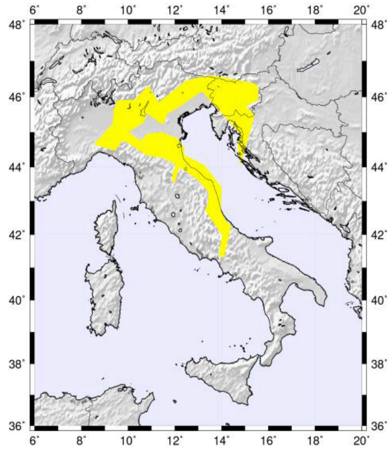

Alerted area based on seismicity analysis
(yellow: CN northern region)

Alerted Areas at National scale

Integrated map of alerted areas

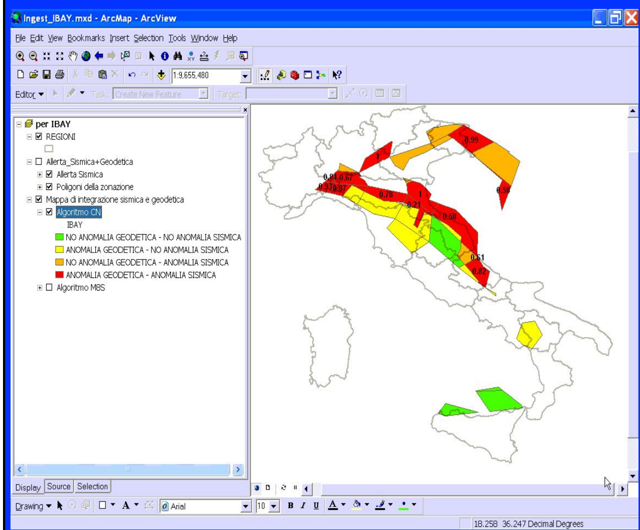

- First fully formalized system for the **joint analysis of strain field** and **seismic stress release**
- Well controlled **prospective testing** and **validation** of the proposed methodologies over the Italian territory.
- **Operational GIS interface:** maps routinely updated and delivered to the Civil Defence every two months

Morphostructural zonation and pattern recognition of earthquake prone areas

Morphostructural zonation and pattern recognition of earthquake prone areas

- **The Morphostructural Zonation method, MSZ *(Alekseevskaya et al., 1977),* allows to identify, independently from earthquake catalogues information, the sites where strong earthquakes are likely to occur.**

Pattern Recognition of Earthquake Prone areas

- Pattern recognition technique is used to identify, **independently from seismicity information**, the sites where strong earthquakes are likely to occur
- **Assumption:** strong events nucleate at the **nodes**, specific structures that are formed around intersections of fault zones.

Pattern Recognition of Earthquake Prone areas

The **nodes** are defined by the **Morphostructural Zonation Method**

↓

delineates a hierarchical block structure of the studied region, based on:

- topography
- tectonic data
- geological data

Pattern Recognition of Earthquake Prone areas

This approach has been applied to many regions of the world. The predictions made in the last 3 decades have been followed by many events (~ 85% of the total) that occurred in some of the nodes previously recognized to be the potential sites for the occurrence of strong events.

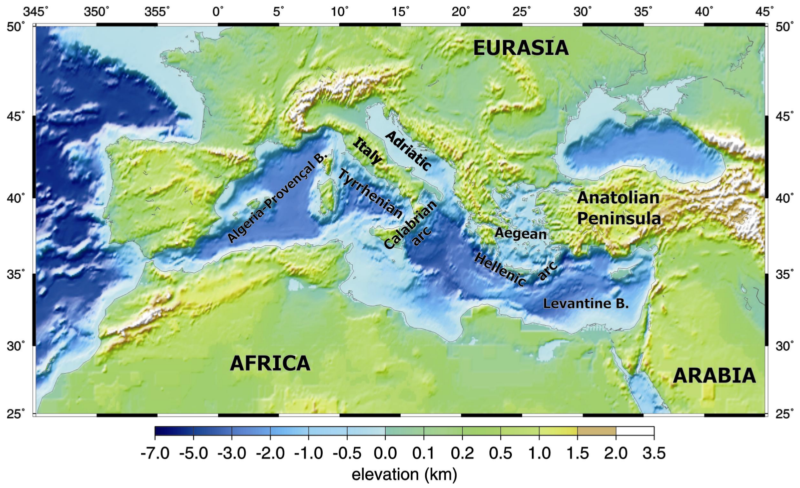

46

Recognition of nodes where strong earthquakes may nucleate in the Mediterranean area

Target magnitudes: ***M*** **$\geq$6.0 - Alps, Apennines and Dinarides**
M **$\geq$5.0 - Iberia**

circles show earthquake-prone nodes
dots mark target earthquakes
yellow marks the nodes where such earthquakes are still unknown

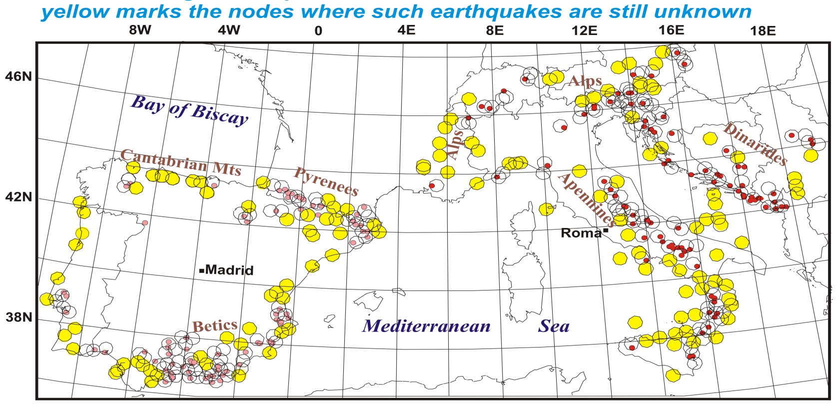

References
Gorshkov A.I., Panza G.F., Soloviev A.A. & Aoudia A. (2002). Morphostructural zoning and preliminary recognition of seismogenic nodes around the Adria margin in peninsular Italy and Sicily. *JSEE:* Spring 2002, 4, No.1, 1-24.
Gorshkov A.I., Panza G.F., Soloviev A.A., Aoudia A. (2004). Identification of seismogenic nodes in the Alps and Dinarides. *Boll.Soc.Geol.Ital.* 123, 3-18.

Multiscale Neo-deterministic Hazard Scenarios

Regional seismic hazard scenarios

(ground motion at bedrock)

- Scenarios associated to alerted CN and M8S regions (+ time)
- Scenarios associated to seismogenic nodes

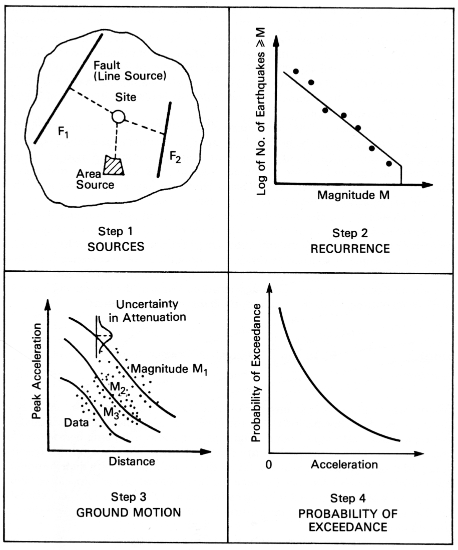

FIGURE 10.2 Basic steps of probabilistic seismic hazard analysis (after TERA Corporation 1978).

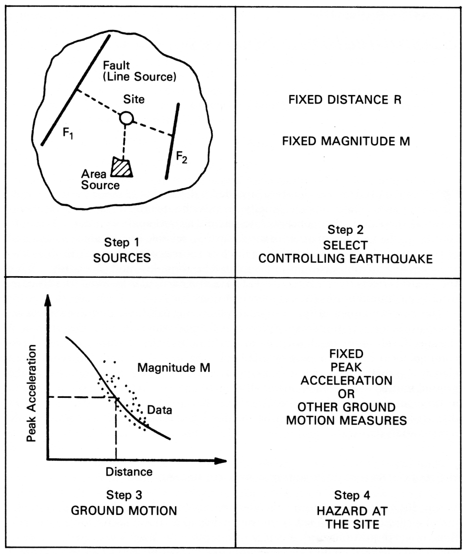

FIGURE 4.1 Basic steps of deterministic seismic hazard analysis (after TERA Corporation 1978).

Probabilistic and Deterministic

procedures after Reiter (1990)

49

Probabilistic

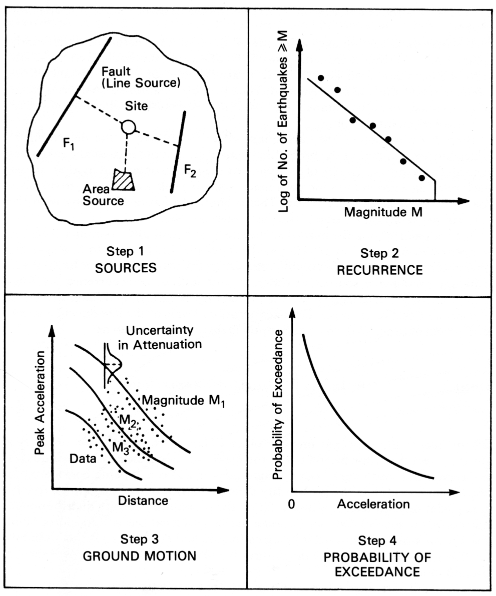

FIGURE 10.2 Basic steps of probabilistic seismic hazard analysis (after TERA Corporation 1978).

Step 2 - Recurrence can be represented by a linear relation only if the size of the study area is large with respect to linear dimensions of sources.

Step 3 - Attenuation relations are not translation invariant in the phase space (M, R, S)), i.e. the relative decay is independent from (M, R, S). Even when translation invariant they are not a conditional probability density function, they represent the functional dependency of the random spectral acceleration on the random variates, M, R and measurement error (Klügel, 2006).

Step 4 - ???

M - magnitude; R - source distance; S - local soil conditions

50

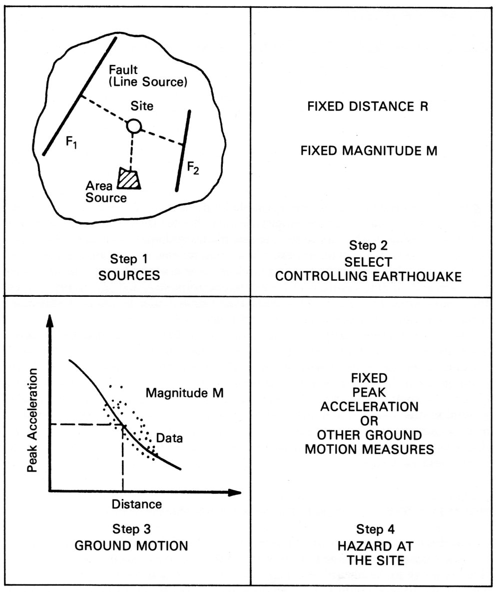

FIGURE 4.1 Basic steps of deterministic seismic hazard analysis (after TERA Corporation 1978).

Deterministic

Step 3 - Most of the attenuation relations are not translation invariant in the phase space (M, R, S)), i.e. the relative decay is independent from (M, R, S). Even when translation invariant they are not a conditional probability density function, they represent the functional dependency of the random spectral acceleration on the random variates, M, R and measurement error (Klügel, 2006).

M - magnitude; R - source distance; S - local soil conditions

51

NEO-DETERMINISTIC

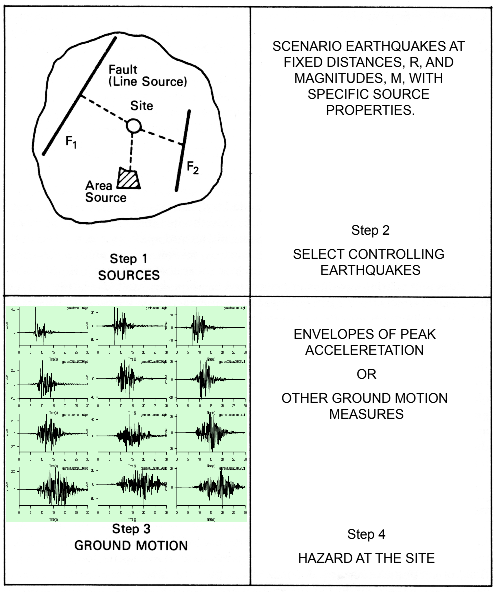

New approach based on synthetic signals computation

No need of attenuation relations

52

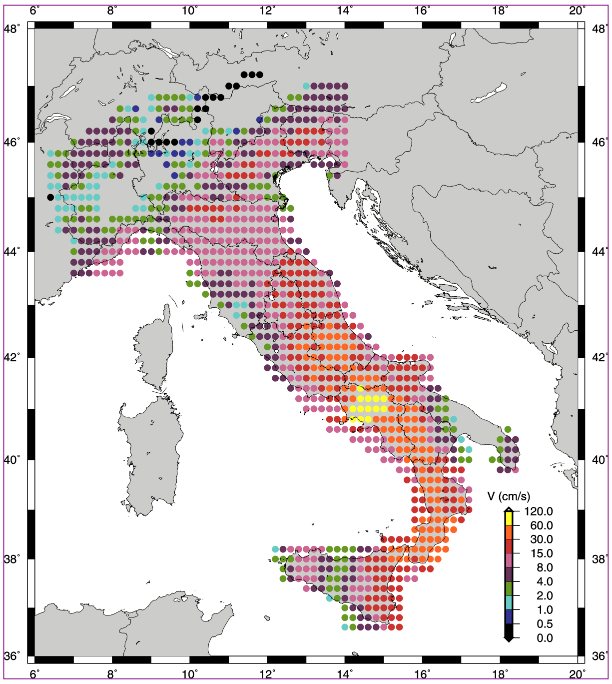

Neo-Deterministic hazard scenarios at national scale Time independent

PGV: Maximum estimated velocity

Scenarios at bedrock

Neo-deterministic Method

Neo-deterministic hazard scenarios associated to alerted regions: M8S algorithm

Prediction of earthquakes with M5.5+

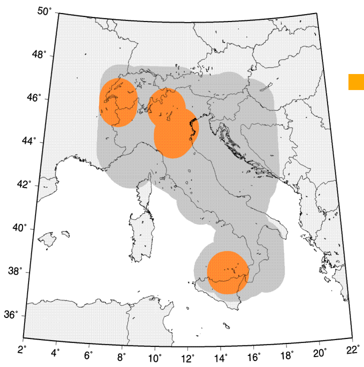

Alerted areas by M8S algorithm
for an earthquake with 5.5≤M<6.0
(as on 1 July 2006 – 1 January 2007)

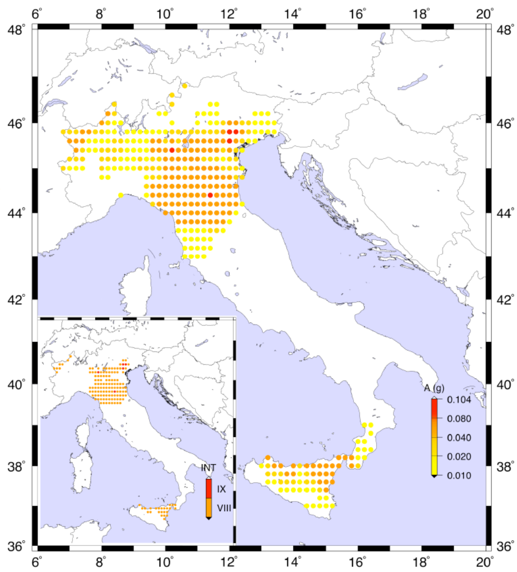

Neo-deterministic hazard scenarios associated to alerted regions: CN algorithm

Northern Region

Prediction of earthquakes with M≥5.4

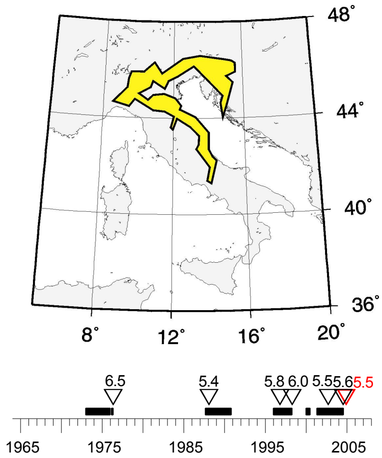

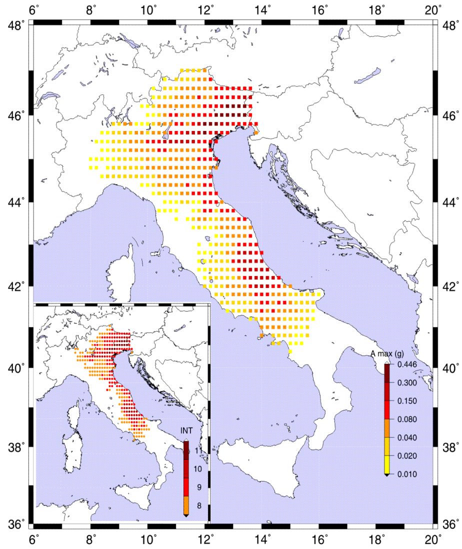

Scenario associated to earthquake prone nodes

Example: node determining the maximum ground motion in the city of

Trieste

corresponding to an earthquake with M=6.5
(compatible with seismic history and seismotectonics)

M≥6.5

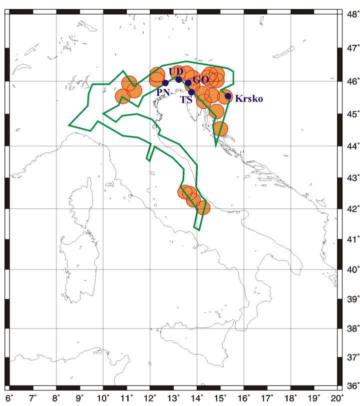

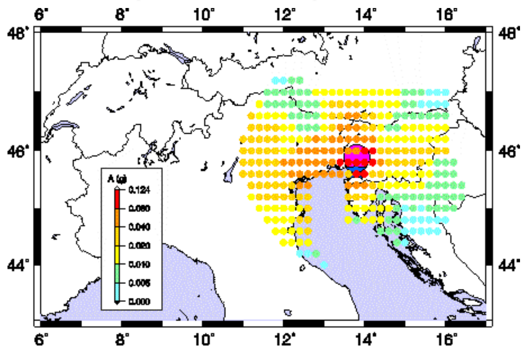

PGD (cm)	PGV (cm/s)	DGA (g)	I_{max} computed ING	I_{max} computed ISG	I_{max} observed
2.0 – 3.5	4.0 – 8.0	0.08-0.15	IX	VIII	VII

Peak Ground Displacement (PGD), Peak Ground Velocity (PGV), Design Ground Acceleration (DGA) and maximum computed intensity (I_{max} computed), estimated using the conversion tables proposed by Panza et al. (2001). The observed intensity in the city of Trieste is the same in the ING and ISG data sets.

April 6, 2009 L'Aquila earthquake

57

The epicenter (★) of L'Aquila earthquake of April 6, 2009 is within an area (red circles) previously identified as capable of earthquakes with M≥6.0, by pattern recognition analysis of morfostructural zonation (MSZ).

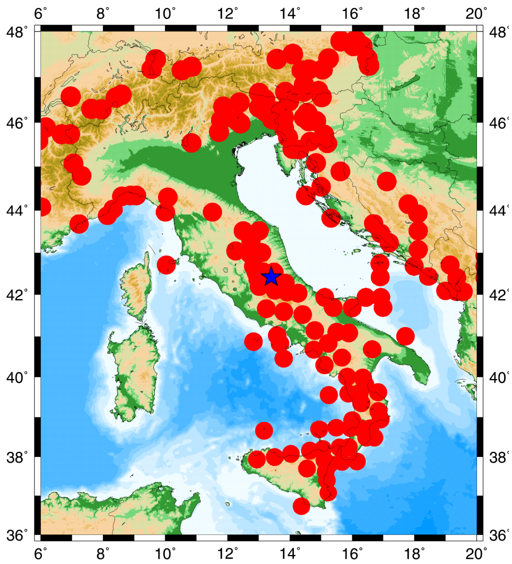

58

On Aprile 6, 2009 a CN alarm was active in the region delineated by the red line; The epicenter of the earthquake falls just outside (about 10 km) the alarmed region.

The earthquake occurred outside of the areas alarmed either by CN or M8S: thus **formallly** it is **a failure to predict**.

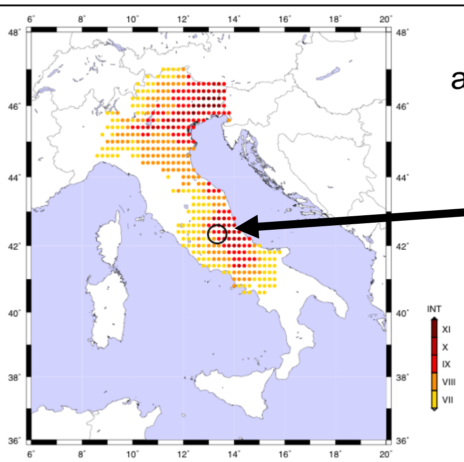

a)

b)

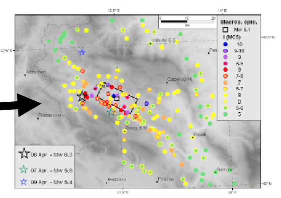

Nevertheless the shaking scenario (seismic ground motion at the bedrock) computed following the alarm has:

(a) correctly predicted the macroseismic intensities observed after the April 6, 2009 event;

(b) supplied information that could have been profitably used by disaster managers.

Multiscale Neo-deterministic Hazard Scenarios

Detailed scenarios of ground motion including local site effects

Modellazioni, basate su di un profilo disponibile in letteratura, mostrano amplificazioni del moto del suolo anche di 10 volte in corrispondenza dei sedimenti alluvionali del fiume Aterno.

Le amplificazioni si manifestano in un ampio intervallo spettrale, ponendo quindi a rischio varie classi di edifici, e spiegano, almeno in parte, la distribuzione a macchia di leopardo dei danni.

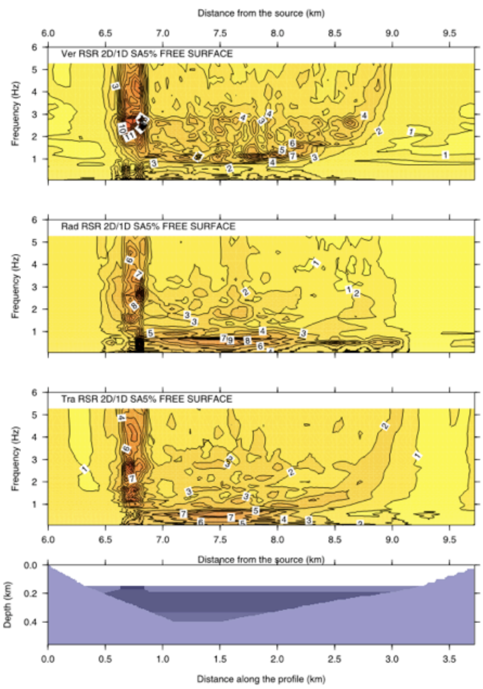

Effects of local soil conditions

Isoseismals shape

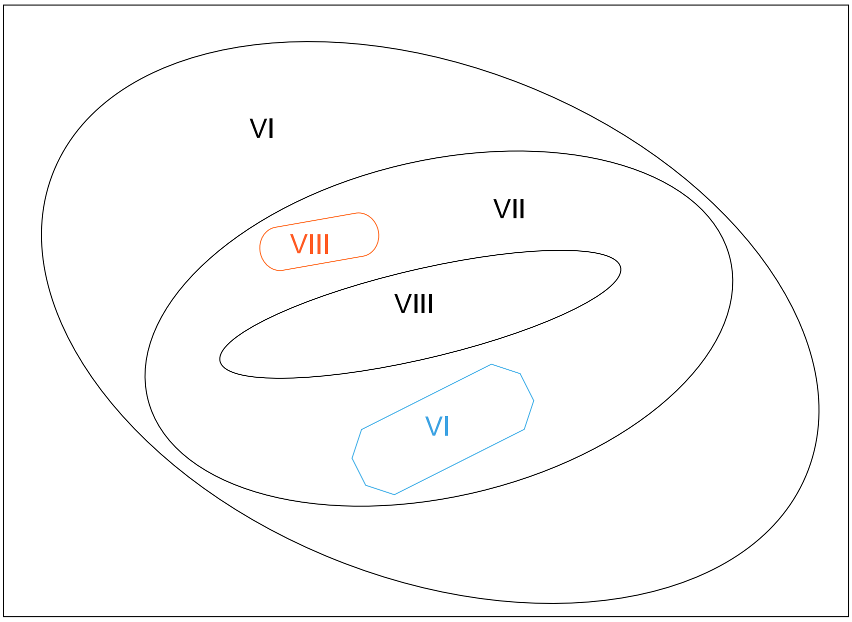

Schematic representation of multi-connected isoseismals (secondary parts in color)

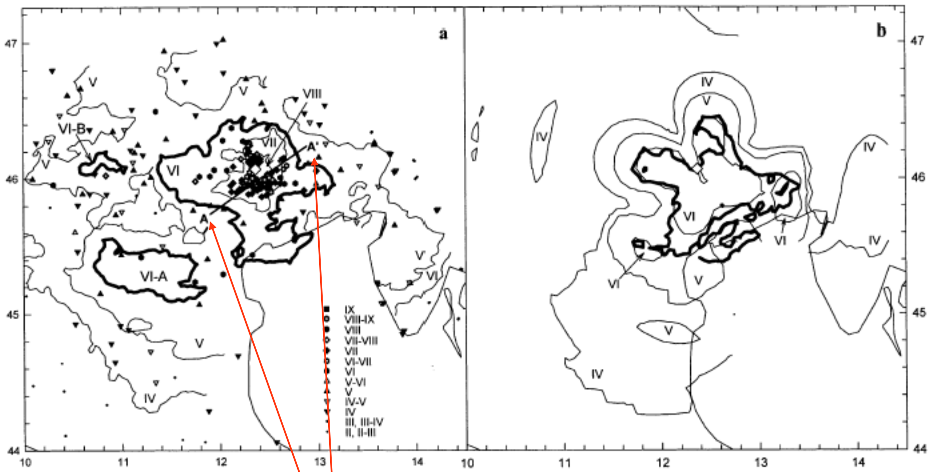

Alpago earthquake (18.10.1936, M_L=5.8): MCS Intensity data (*point-like symbols*) and isolines defined with polinomial filtering; segment (A, A') separates the zone with I≥VI on mountain from that on plain. Areas VI-A e VI-B are local effects?

(b) isolines of the synthetic a_p-field (*thin line*) and reconstruction of the theoretical I_a=VI isoline (*bold line*) using the original observation points and the polynomial filtering technique (Molchan et al., 2002, PAGEOPH, 159).

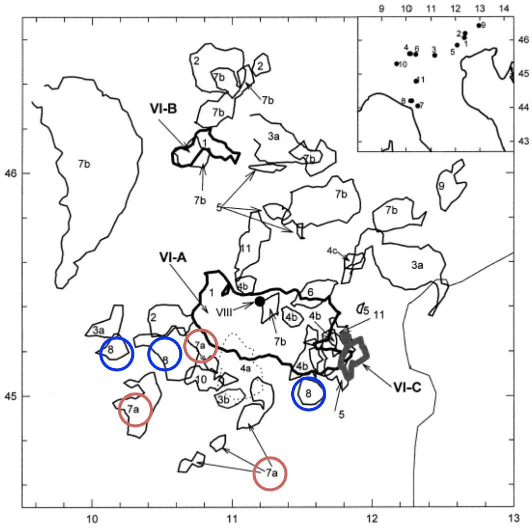

1) 18.10.1936, Alpago, V+1 (*think line*; VI-A, VI-B), area VI-C is an alternative to the area VI-A due to instability of the the polynomial.
2) 29.06.1873, Bellunese, V+1 (2).
3) 7.06.1891, Veronese, IV+1 (3a), V+1 (3b).
4) 27.11.1894, Franciacorta, IV-1 (4a, *dotted line*), III+1 (4b), II+1 (4c).
5) 4.03.1900, Valdobbiadene, IV+1 (5).
6) 30.10.1901, Salo, IV+1 (6).
7) 27.10.1914, Garfagnana, V+1 (7a), IV+1 (7b).
8) 7.09.1920, Garfagnana, IV+1 (8).
9) 12.12.1924, Carnia, IV+1 (9).
10) 15.05.1951, Lodigiano, V+1 (10).
11) 15.07.1971, Parmense, IV+1 (11).

Secondary parts (*thin line*) of the multi-connected isoseismals for the 11 earthquakes in the zone of Alpago earthquake.

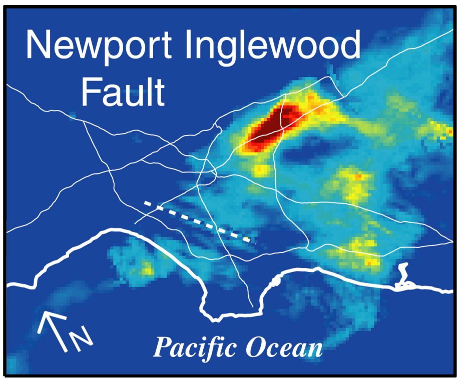

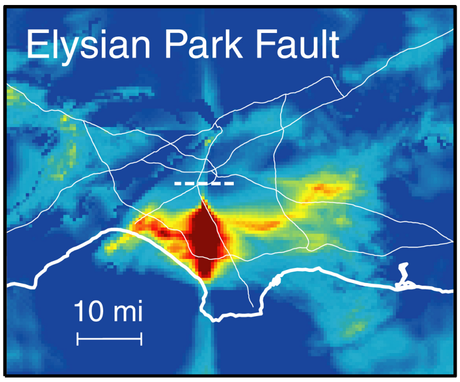

These images of the Los Angeles Basin show "hotspots" predicted from computer simulations of an earthquake on the Elysian Park Fault and an earthquake on the Newport-Inglewood Fault (represented by the white dashed lines). What is shown is **not** how much shaking was experienced at a particular site but rather how much more or less shaking (highest levels are shown in red) a site receives **relative to what is expected** from only the magnitude of the earthquake and the site's distance from the fault. These images consider only part of the total shaking (long-period motions) and were calculated by using a simplified geologic structure. (Data for images courtesy of Kim Olsen, University of California, Santa Barbara, SCEC Phase III report).

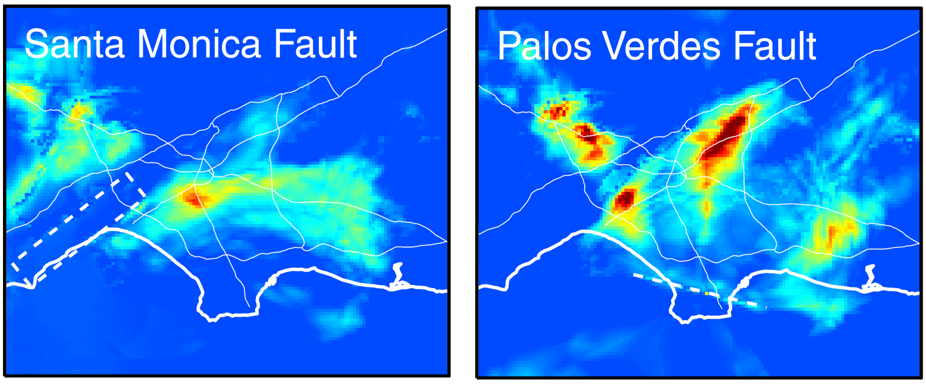

"hotspots" predicted from computer simulations of an earthquake on the Santa Monica Fault and an earthquake on the Palos Verdes Fault (represented by the white dashed lines). SCEC Phase III report, Field, 2000, BSSA, see also http://www.scec.org/phase3/

Hot/Cold Spots in Italian Macroseismic Data

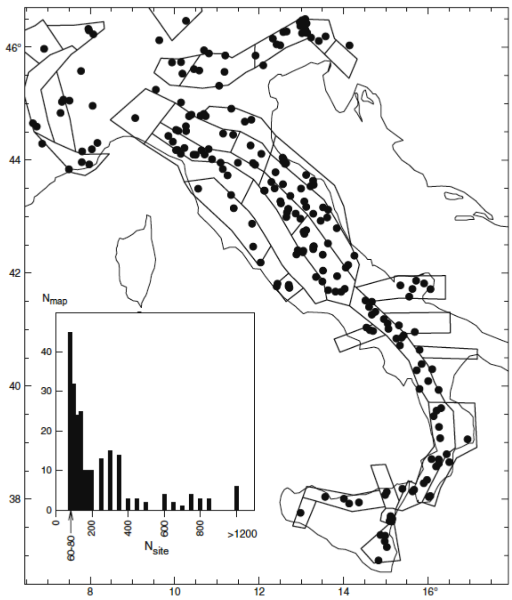

Figure 1

Earthquakes selected for the analysis of *I*-maps. The *inset* shows the number of maps (N_{map}) with given number of sites (N_{site}). The *thin lines* show the seismic source zones by Meletti *et al.* (2008)

G. Molchan et al. Pure Appl. Geophys.

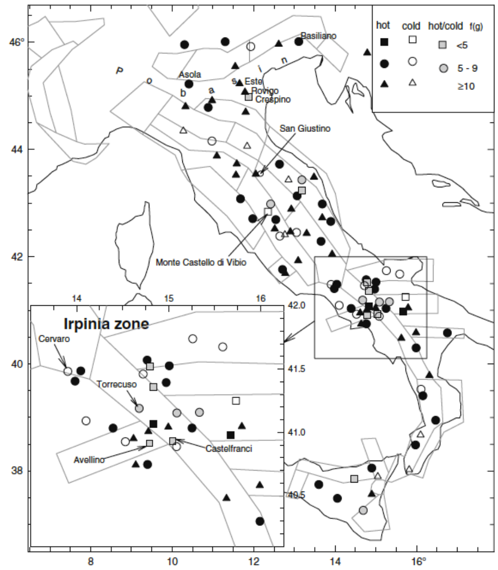

Figure 4
Anomalous sites of three types (hot, cold, hot/cold) and their characteristic $f(g)$; the *thin lines* show the seismic source zones by MELETTI *et al.* (2008)

Hot/Cold Spots in Italian Macroseismic Data

Table 1

Anomalous sites and their characteristics

#	Site g_0 (province)	Coordinates Lat	Long	Type $s(g_0)$	$f(g) = N_{map}/N_s$	I-Map* EQ date	I_0	Dist	$I(g_0)$	$\Delta I(g_0)$
1	Accadia (FG)	41.158	15.334	±	14/2	1990.05.05	7	49	4.5	+1
						1984.05.07	8	137	5	–1
2	Acquasparta (TR)	42.690	12.546	+	10/2	1984.05.11	7	175	4	+1
						1984.04.29	7	65	5	+1
3	Altavilla Irpina (AV)	41.006	14.779	+	10/1	1984.05.07	8	110	5	+1
4	Anghiari (AR)	43.540	12.054	+	13/1	1920.09.07	9.5	173	5	+1
5	Ariano Irpino (AV)	41.153	15.089	+	18/1	1456.12.05	11	52	9.5	+1
6	Asola (MN)	45.221	10.413	+	10/2	1920.09.07	9.5	112	5.5	+1
						1987.05.02	6	55	5	+1
7	Asolo (TV)	45.801	14.791	+	12/1	1987.05.02	6	137	4	+1
8	Avellino (AV)	40.914	14.791	±	24/6	1732.11.29	9.5	24	9	+1
						1805.07.26	10	74	8	+1
						1889.12.08	7	120	2.5	–1
						1980.11.23	9.5	40	8	+1
						1982.03.21	7.5	149	5	+1
						1984.05.07	8	119	5	+1
9	Bagaladi (RC)	38.026	15.821	–	12/1	1783.03.28	10	93	5	–1
10	Baiano (AV)	40.951	14.618	+	11/1	1910.06.07	9	68	7	+1.5
11	Baronissi (SA)	40.746	14.770	+	9/1	1910.06.07	9	54	7	+1
12	Baselice (BN)	41.393	14.973	+	9/1	1991.05.26	7	118	4.5	+1
13	Basiliano (UD)	46.013	13.109	+	8/1	1988.02.01	6	27	5.5	+1
14	Breno (BS)	45.956	10.303	+	9/1	1936.10.18	9	161	6	+1
15	Brienza (PZ)	40.478	15.628	+	10/1	1905.09.08	11	210	6	+1
16	Caltanissetta (GL)	37.490	14.057	+	8/1	1990.12.13	7.5	89	5.5	+1
17	Camerino (MC)	43.135	13.068	+	28/3	1980.11.23	9.5	338	5	+1
						1984.05.07	8	190	4	+1
						1984.05.11	7	189	4	+1
18	Campli (TE)	42.726	13.686	+	13/1	1984.05.07	8	124	5	+1
19	Cantalice (RI)	42.466	12.904	+	13/1	1987.07.03	7	87	4	+1
20	Capizzi (ME)	37.848	14.479	±	9/2	1905.09.08	11	157	6	+1
						1908.12.28	11	104	4	–1
21	Carpi (MO)	44.784	10.885	+	17/2	1919.06.29	9	111	6	+2
						1920.09.07	9.5	77	6	+1
22	Cassano allo Ionio (CS)	39.784	16.317	+	10/1	1980.11.23	9.5	162	6	+1
23	Castel Giorgio (TR)	42.708	11.979	+	7/1	1993.06.05	6	69	5	+1.5
24	Castelfranci (AV)	40.931	15.043	±	8/2	1990.05.05	7.0	37	6.5	+1.5
						1991.05.26	6.5	76	1	–2
25	Cercemaggiore (CB)	41.460	14.722	–	9/1	1688.06.05	11	21	6	–1
26	Cervaro (FR)	41.481	13.904	–	8/1	1915.01.13	11	75	5	–1.5
27	Collagna (RE)	44.347	10.275	–	18/1	1920.09.07	9.5	15	7	–1
28	Colle Sannita (BN)	41.361	14.833	+	13/2	1984.05.07	8	86	6	+1
						1984.05.11	7	83	6	+1
29	Concordia sulla Secchia (MO)	44.914	10.981	+	10/2	1891.06.07	9	72	6	+1
						1971.07.15	7.5	46	7	+1
30	Contigliano (RI)	42.411	12.769	–	14/1	1979.09.19	8	39	4.5	–1
31	Cossignano (AP)	42.983	13.688	+	7/1	1915.01.13	11	104	7.5	+1
32	Crespino (RO)	44.982	11.885	+	7/1	1987.05.02	6	93	5	+1
33	Deruta (PG)	42.982	12.420	±	14/2	1930.10.30	8.5	93	5	+1
						1998.03.26	6.5	57	4	–1
34	Este (PD)	45.228	11.656	+	15/1	1914.10.27	7	134	6	+1
35	Ginosa (TA)	40.578	16.758	+	7/1	1905.09.08	11	209	6	+1
36	Grazzanise (CE)	41.091	14.102	+	8/1	1984.05.07	8	68	5	+1
37	Jelsi (CB)	41.518	14.796	±	8/2	1915.01.13	11	129	6.5	+1.5
						1980.11.23	9.5	90	4	–1

G. Molchan et al. Pure Appl. Geophys.

Table 1 continued

#	Site g_0 (province)	Coordinates Lat	Long	Type $s(g_0)$	$f(g) = N_{map}/N_s$	I-Map* EQ date	I_0	Dist	$I(g_0)$	$\Delta I(g_0)$
38	Lavello (PZ)	41.046	15.795	+	10/1	1857.12.16	10.5	75	4	+1
39	Lercara Friddi (PA)	37.748	13.603	+	7/1	1908.12.28	11	180	7	+1
40	Levico Terme (TN)	46.011	11.303	+	8/1	1976.12.13	7	38	6	+1
41	Marcianise (CE)	41.033	14.395	+	7/1	1915.01.13	11	139	7	+1
42	Micigliano (RI)	42.451	13.054	–	9/1	1915.01.13	11	63	5	–1
43	Miglierina (CZ)	38.947	16.471	+	7/1	1990.05.05	7	237	4	+1
44	Mignano Monte Lungo (CE)	41.404	13.983	+	8/1	1980.11.23	9.5	132	7	+1
45	Mineo (CT)	37.266	14.691	±	10/2	1905.09.08	11	186	5	+3
						1980.01.23	5.5	43	2	–1
46	Mirabella Elcano (AV)	41.042	14.996	+	13/1	1980.11.23	9.5	33	8	+1
47	Moio Alcantara (ME)	37.899	15.051	–	11/3	1905.09.08	11	117	3	–1
						1908.12.28	11	57	5	–1
						1975.01.16	7	53	1	–1
48	Mongrassano (CS)	39.526	16.111	–	7/1	1908.12.28	11	152	5	–1
49	Montalto Uffugo (CS)	39.405	16.158	+	9/1	1990.05.05	7	174	5.5	+1.5
50	Monte Castello di Vibio (PG)	42.840	12.352	–	8/2	1993.06.05	6	39	1	–1
						1997.09.26	9	45	4	–1
51	Monteleone, (VV) Vibo Valentia	38.675	16.102	–	10/1	1638.03.27	11	45	6.5	–1
52	Montemurro (PZ)	40.297	15.991	+	10/2	1905.09.08	11	181	6	+1
						1980.11.23	9.5	95	7	+1
53	Montevarchi (AR)	43.523	11.568	+	18/1	1915.01.13	11	246	6	+2
54	Narni (TR)	42.517	12.521	+	19/1	1998.08.15	6	47	4	+1
55	Nocera Inferiore (SA)	40.743	14.642	+	15/1	1991.05.26	6.5	100	4.5	+1
56	Nola (NA)	40.926	14.529	–	12/2	1688.06.05	11	37	5	–1
						1991.05.26	6.5	117	1	–1.5
57	Notaresco (TE)	42.657	13.894	+	9/1	1984.05.07	8	112	6	+2
58	Nusco (AV)	40.887	15.085	–	8/1	1930.07.23	10	25	5	–1
59	Osimo (AN)	43.485	13.483	+	22/1	1741.04.24	9	39	8	+1
60	Parma (PR)	44.801	10.329	+	25/1	1989.10.03	4	35	3	+2
61	Paternò (CT)	37.566	14.902	+	13/1	1905.09.08	11	151	6	+1
62	Pienza (SI)	43.079	11.679	+	8/1	1993.06.05	6	81	3	+2
63	Pizzoli (AQ)	42.435	13.303	+	11/1	1933.09.26	9	78	7	+1
64	Porcia (PN)	45.964	12.618	+	10/1	1976.05.06	9.5	46	8	+1
65	Porretta (BO)	44.156	10.976	–	12/2	1909.01.13	6.5	74	3	–1
						1920.09.07	9.5	60	4	–1
66	Portomaggiore (FE)	44.697	11.805	+	13/1	1916.05.17	7.5	105	6	+1
67	Prato (PO)	43.879	11.096	+	22/1	1983.11.09	6.5	123	5	+1
68	Quero (BL)	45.921	11.931	–	7/1	1895.04.14	8.5	169	4	–1
69	Raccuja (ME)	38.055	14.901	+	7/1	1905.09.08	11	115	7	+1
70	Rapolla (PZ)	40.976	15.675	+	7/2	1990.05.05	7	37	7	+1
						1991.05.26	6.5	41	6.5	+1
71	Rignano Garganico (FG)	41.675	15.587	–	8/1	1962.08.21	9	69	4	–2
72	Rocca di Papa (RM)	41.760	12.710	+	12/2	1898.06.27	7.5	71	5	+1
						1995.06.12	5.5	24	5	+1
73	Rocca San Casciano (FC)	44.060	11.842	–	17/1	1920.09.07	9.5	131	1	–2
74	Rosarno (RC)	38.487	15.978	+	9/1	1894.11.16	8.5	23	8	+1
75	Rovigo (RO)	45.070	11.790	+	15/1	1983.11.09	6.5	114	5	+1
76	San Marco la Catola (FG)	41.525	15.006	+	9/1	1995.09.30	6	52	5.5	+1
77	San Martino Sannita (BN)	41.066	14.837	+	7/2	1805.07.26	10	60	8	+1
						1990.05.05	7	61	6.5	+1
78	San Paolo di Civitate (FG)	41.739	15.261	–	8/1	1980.11.23	9.5	101	4	–1
79	San Pio delle Camere (AQ)	42.286	13.656	+	7/1	1990.05.05	7	242	4	+1

Hot/Cold Spots in Italian Macroseismic Data

Table 1 continued

#	Site g_0 (province)	Coordinates		Type $s(g_0)$	$f(g) = N_{map}/N_s$	*I*-Map*				
		Lat	Long			EQ date	I_0	Dist	$I(g_0)$	$\Delta I(g_0)$
80	San Severino Marche (MC)	43.229	13.177	±	18/4	1972.11.26	7.5	44	4	−1
						1980.11.23	9.5	341	5	+1
						1987.07.03	7	40	6	+1
						1993.06.05	6	39	2	−1
81	Sassoferrato (AN)	43.434	12.858	−	22/1	1984.04.29	7	32	4	−1
82	Sellano (PG)	42.888	12.926	+	20/1	1987.07.03	7	59	5	+1
83	Staffolo (AN)	43.432	13.186	±	12/2	1741.04.24	9	18	5.5	−1
						1979.09.19	8	78	6	+1
84	Stornarella (FG)	41.256	15.731	−	8/2	1913.10.04	7.5	96	1	−1.5
						1991.05.26	6.5	71	3	−1
85	Subiaco (RM)	41.925	13.095	+	19/1	1979.09.19	8	91	6	+1
86	Sulmona (AQ)	42.047	13.928	+	23/2	1933.09.26	9	18	8	+1
						1987.07.03	7	127	6	+2
87	Toro (CB)	41.570	14.766	+	7/1	1990.05.05	7	114	4.5	+1
88	Torrecuso (BN)	41.189	14.679	±	10/2	1991.05.26	6.5	121	5	+2
						1990.05.05	7	82	1	−3
89	Trivigno (PZ)	40.580	15.990	+	10/1	1905.09.08	11	213	6	+1
90	Urbino (PU)	43.726	12.636	+	35/4	1873.03.12	7.5	78	6.5	+1
						1904.11.17	7	122	3	+2
						1907.01.23	5.5	154	3.5	+2
						1915.01.13	11	212	6	+1
91	Vacone (RI)	42.384	12.644	−	8/1	1979.09.19	8	47	4	−1
92	Vallata (AV)	41.034	15.253	+	8/1	1991.05.26	6.5	69	5.5	+1
93	Vallombrosa (FI)	43.731	11.588	+	10/1	1914.10.27	7	94	6	+1
94	Velletri (RM)	41.688	12.778	+	13/1	1990.05.05	7	255	3.5	+1.5
95	Venafro (IS)	41.485	14.044	+	15/2	1997.03.19	6	65	3	+2
						1990.05.05	7	149	6.5	+1.5
96	Vicenza (VI)	45.549	11.549	+	14/1	1983.11.09	6.5	119	5	+1

* *EQ* earthquake; I_0 intensity at epicenter, *dist* distance from g_0 in km

- The use of modelling is necessary because, contrary to the common practice, the so-called local site effects cannot be modelled by a convolutive method, since they can be ***strongly dependent upon the properties of the seismic source***.

- The wide use of realistic synthetic time histories, **which model the waves propagation from source to site**, allows us to easily construct scenarios based on significant ground motion parameters (acceleration, velocity and displacement).

WHY?

Formal problem

About convolutive/deconvolutive methods

In the far field (and in the point source approximation, i.e. in the simplest possible case) the displacement (the seismogram) is:

$u_k(t)=\Sigma_{ij}M_{ij}(t)*G_{ki,j}(t)$

k, i and j are indices and ,j means derivative, * means convolution, G is the Green's function and M_{ij} are moment tensor rate functions.

If we constrain the independence of M_{ij} and ask for a constant mechanism (even unconstrained one, i.e. the full moment tensor), i.e. if we impose the constraint

$$M_{ij}(t)=M_{ij}.m(t)$$

the problem becomes non-linear.

In fact in the product $M_{ij}.m(t)$ on the right-hand side of:

$$u_k(t)=M_{ij}.m(t)*G_{ki,j}(t)$$

both M_{ij} and $m(t)$ are model parameters controlling source properties. There is no problems if the source force is a singlet.

In the frequency domain it may seem simpler because the above convolution is converted to pure multiplication:

$$u_k(\omega)=M_{ij}(\omega) \cdot G_{ki,j}(\omega)$$

and the equation is solved for each frequency separately. Within linearity we get $M_{ij}(\omega)$ but to split the source time function and the mechanism again a non-linear constraint is needed, so the advantage of the frequency domain is fictitious only.

Good news towards implementation - 1

An agreement has been renewed among the Abdus Salam International Centre for Theorethical Physics, ICTP, and the Civil Defence of the Friuli Venezia Giulia Region (NE Italy) for the practical implementation of the integrated neo-deterministic hazard procedure.

Routinely updated time dependent seismic hazard maps are made available to the Civil Defence (end user).

Good news towards implementation - 2

Resolution of Italian Parliament n. 8/00124, Legislatura 16, approved on 8 June 2011, Bollettino della Camera dei Deputati, n. 491, All. 5, pp. 388-393, that endorses the use of NDSHA as a validation tool of PSHA.

Glaciation and earthquakes

84

Snow load effect on seimicity

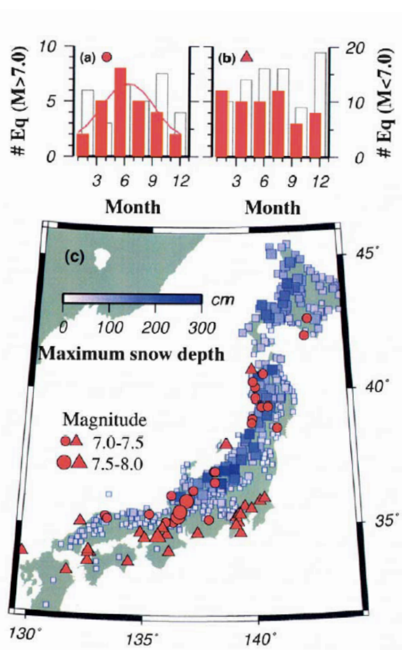

Number of earthquakes occurred in 2-month intervals, within (a) and outside (b) the snowy region. Red and white histograms show M≥7.0 (left) and 7.0>M≥6.0 (right) events, respectively. In (c) blue squares show maximum snow depths in a winter at AMeDAS stations (only points with snows deeper than 20.0 cm are shown). Epicenters of M≥7.0 earthquakes are shown in (c) as circles (snowy region) and triangles (outside). Red curve in (a) is the best-fit probability density function of the earthquake occurrence based on the two-component (stationary and annual) model (Heki, EPSL, 2003).

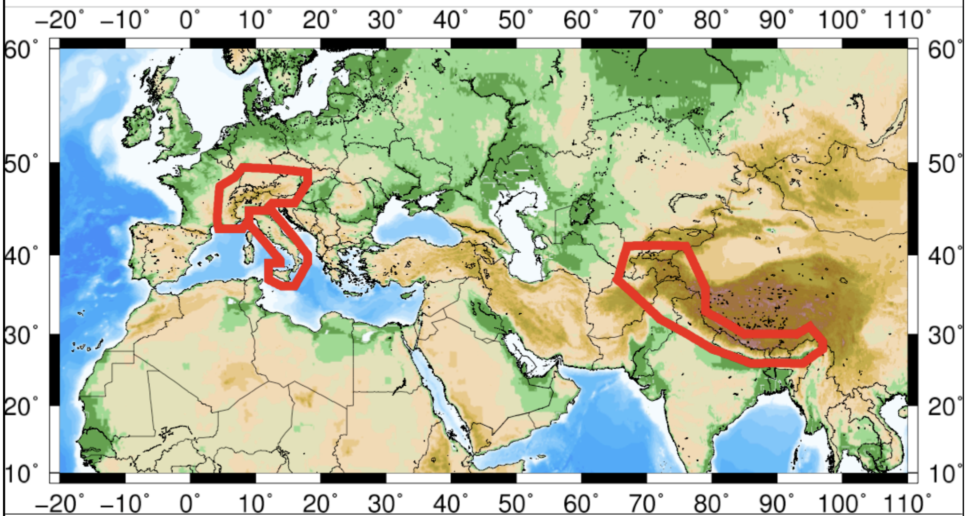

Study regions: Apennines, Alps, Himalaya

87

Seismicity is quantified by means of N (number of events) and Σ. Σ is based on Benioff strain release (Benioff, 1951) S_i, computed for each earthquake *i* with magnitude M_i, and normalized to the strain S_{min} of the minimum magnitude M_{min} considered for the analysis, that is:

$$\Sigma = \sum_i \frac{S_i}{S_{min}} = \sum_i 10^{\frac{d}{2}(M_i - M_{min})}$$

where for the constant *d* we use the value *d*=1.5 given by Gutenberg and Richter (1956).

88

Seasonal modulation of seismicity

Tectonic forces responsible for mountain building in compressional regimes must overcome, among others, gravity

➡ Possibility for competing effects of tectonic forces and the load due to snow and ice cover

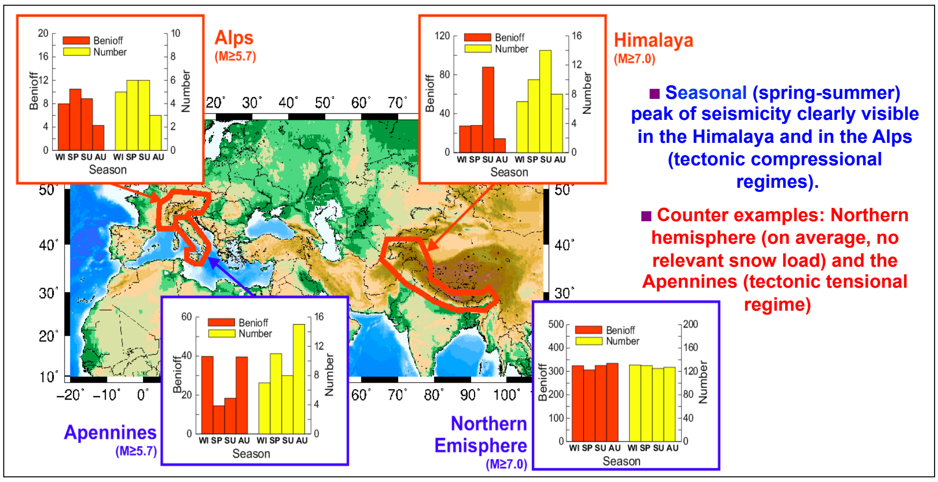

(Panza, Peresan & Zuccolo, Terra Nova 2010)

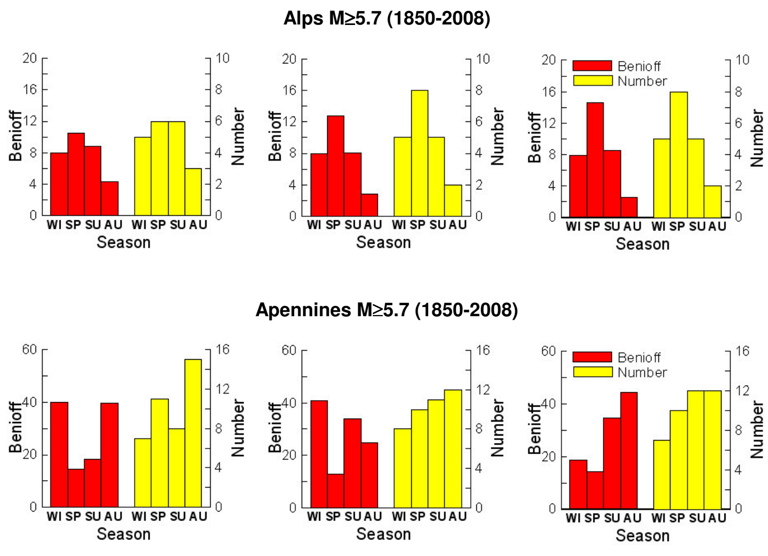

Figure 1 - Histograms of Σ and N for the crustal events which occurred in the b) Alps and d) Apennines. The three columns correspond to winter starting on 1 December, 15 December and 31 December, respectively.

90

ALPS + APENNINES

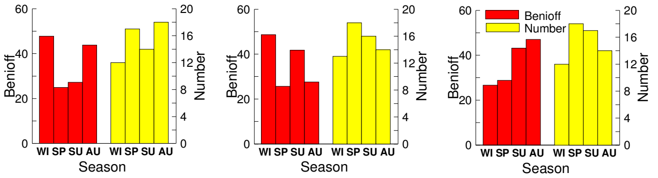

b) CUMULATIVE – SHIFT IN APENNINES

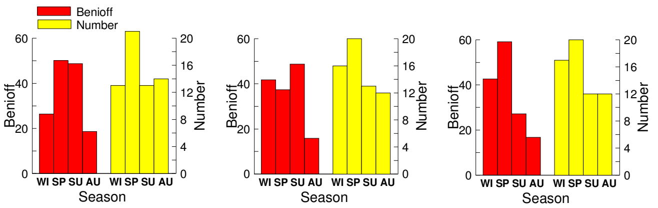

Figure 2 - Histograms of Σ and N for the crustal events, which occurred in the Alps and in the Apennines. The three columns correspond to winter starting on 1 December, 15 December and 31 December, respectively.

Values correspond, in each column, to the average sum of Σ and N from Alps and Apennines,.as given in Fig. 1. The values are computed: a) without seasonal shift between Alps and Apennines; b) with seasonal shift in the Apennines, so as the following intervals are summed up:

Alps	SU	AU	WI	SP
Appenines:	WI	SP	SU	AU

ALPS (percentage)

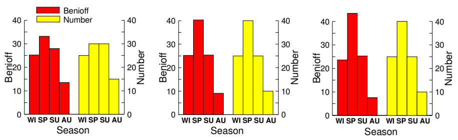

APENNINES (percentage)

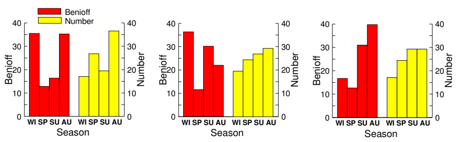

Figure 3 - Histograms of Σ and N for the crustal events which occurred in the b) Alps and d) Apennines. The three columns correspond to winter starting on 1 December, 15 December and 31 December, respectively.

Values are expressed in percentage of the total Σ and N during the year.

a) CUMULATIVE – NO SHIFT (percentage)

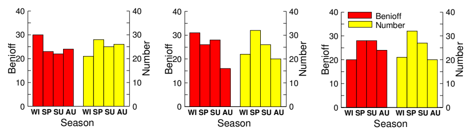

b) CUMULATIVE – SHIFT IN APENNINES (percentage)

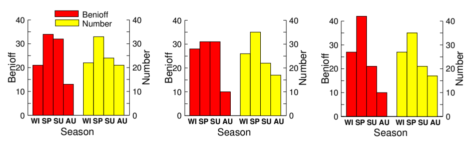

Figure 4 - Histograms of Σ and N for the crustal events, which occurred in the Alps and in the Apennines. The three columns correspond to winter starting on 1 December, 15 December and 31 December, respectively.

Values correspond, in each column, to the average (sum/2) of the percentages from Alps and Apennines,.as given in Fig. 2. The values are computed: a) without seasonal shift between Alps and Apennines; b) with seasonal shift in the Apennines, so as the following intervals are summed up:

Alps	SU	AU	WI	SP
Appenines:	WI	SP	SU	AU

Normalized quantities are used to give the same weight to Alps and Apennines seismicity

Effect of past temperatures and climate changes on seismicity

93

Secular modulation of seismicity

- A **significant secular modulation of seismicity** is detected in the Himalaya and the Alps, two regions characterized by present day mountain building and relevant glaciers retreat.
- Seismicity modulation can be **correlated with surface atmosphere temperature changes** in Northern hemisphere over the last ten centuries.

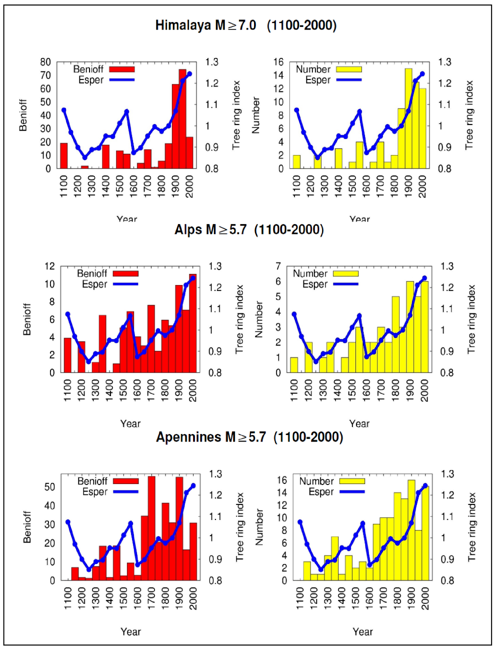

Histograms of seismicity and average surface atmosphere temperature variation in the Northern hemisphere (Esper et al., 2002)

(Panza, Peresan & Zuccolo, Terra Nova 2010)

Quantitative estimate of the statistical significance of the correlation between seismicity and temperature variation.

Spearman correlation coefficient between seismicity (Σ and N) and average surface atmosphere temperature estimated for different time intervals. The confidence level is ≥ 95% (p-value, given in parenthesis, is ≤ 0.05) in the Alps and Himalaya.

Region	Σ since 1100	N since 1100	Σ since 1500	N since 1500
Himalaya	0.79 (<0.01)	0.69 (<0.01)	0.79 (0.01)	0.78 (0.01)
Alps	0.51 (0.03)	0.49 (0.03)	0.66 (0.03)	0.60 (0.05)
Apennines	0.20 (0.41)	0.29 (0.24)	-0.14 (0.69)	0.21 (0.54)

95

Conclusions

- **The neo-deterministic seismic hazard procedure makes it possible the combined use of wide geophysical and geological data sets, knowledge of the physical process of earthquake generation and wave propagation in realistic anelastic media, and does not need to rely only on macroseismic observations, the key basis for most earthquake catalogues.**

Conclusions

- **The neo-deterministic hazard assessment and the recognition of earthquake prone areas procedures are especially useful as a mean of prevention in areas where historical and instrumental information is scarce.**

Conclusions

- **The seismic input (complete seismograms) provided by the realistic modeling of ground motion permits the engineering non-linear dynamic analysis of relevant structures (e.g. bridges, hospitals, dams) (*Field et al., 2000*).**

Conclusions

- **Fully formalized algorithms for intermediate-term middle range earthquake predictions are currently available for the routine monitoring of seismicity. The real-time monitoring of seismic flow allows for the forward testing of CN and M8S predictions.**

Conclusions

- **Pattern recognition techniques, earth observations and neo-deterministic seismic hazard procedures can be integrated, blending together the available information in a set of time-dependent neo-deterministic scenarios of ground motion regional and local scale.**

Conclusions

- One of the advantages of the proposed approach consists in the time information provided by intermediate-term predictions, that supply decision makers an objective tool indicating priorities for timely mitigation actions (e.g. retrofitting of critical structures).

Selected References 1

- Gorshkov, A.I., Kossobokov V., Soloviev A. (2002a) - Recognition of earthquake prone areas. In: (Edts., V. Keilis-Borok & A. Soloviev) Nonlinear Dynamics of the Lithosphere and Earthquake Prediction. Springer, Heidelberg, 235-320.
- Gorshkov, A.I., Panza G.F., Soloviev A.A. and Aoudia A., (2002b). Morphostructural Zonation and Preliminary Recognition of Seismogenic Nodes Around the Adria Margin in Peninsular Italy and Sicily. Journal of Seismology and Earthquake Engineering, 4, 1-24.
- Gorshkov, A.I., Panza, G.F., Soloviev, A.A. and Aoudia, A., (2004). Identification of seismogenic nodes in the Alps and Dinarides. Boll. Soc. Geol. It., 123, 3-18.
- Keilis-Borok, V.I., Kossobokov, V.G., (1987). Periods of high probability of occurrence of the world's strongest earthquakes, Computational Seismology 19, Allerton Press Inc., pp. 45-53.

Selected References 2

- Keilis-Borok, V.I., and Kossobokov, I.M. (1990) – Premonitory activation of earthquake flow: algorithm M8. Phys. Earth Planet. Inter. 61, 73-83.
- Keilis-Borok, V.I., Rotwain, I.M., (1990). Diagnosis of time of increased probability of strong earthquakes in different regions of the world: algorithm CN. Phys. Earth Planet. Inter. 61, 57-72.
- Kossobokov, V.G, Romashkova, L.L., Panza, G.F. and Peresan, A., (2002). Stabilizing Intermediate-Term Medium-Range Earthquake Predictions. JSEE, 4, 11-19.
- Molchan, G.M., Kronrod, T.L., Panza, G.F., (1997). Multiscale seismicity model for seismic risk. Bull. Seismol. Soc. Am. 87, 5, 1220-1229.
- Panza, G.F., Romanelli, F. and Vaccari, F., (2001). Seismic wave propagation in laterally heterogeneous anelastic media: theory and applications to seismic zonation. Advances in Geophysics, 43, 1-95.

Selected References 3

- Panza, G.F., Alvarez, L., Aoudia, A., Ayadi, A., Benhallou, H., Benouar, D., Bus, Z., Chen, Y., Cioflan, C., Ding, Z., El-Sayed, A., Garcia, J., Garofalo, B., Gorshkov, A., Gribovszki, K., Harbi, A., Hatzidimitriou, P., Herak, M., Kouteva, M., Kuznetzov, I., Lokmer, I., Maouche, S., Marmureanu, G., Matova, M., Natale, M., Nunziata, C., Parvez, I.A., Paskaleva, I., Pico, R., Radulian, M., Soloviev, A., Suhadolc, P., Szeidovitz, G., Triantafyllidis, P. and Vaccari. F., (2002). Realistic modeling of seismic input for megacities and large urban areas (the UNESCO/IUGS/IGCP project 414). Episodes, 25-3, 160-184.
- Panza, G.F., Peresan, A., Vaccari, F., Romashkova, L., Kossobokov, V., Gorshkov, A. and Kuznetsov, I., (2003). Earthquake preparedness: the contribution of earthquake prediction and deterministic hazard research. IEC Terratremols i temporals de llevant: dos exemples de sistemes complexos, 15, 91-116.
- Panza, G.F., Peresan, A., Romanelli, F., Vaccari, F., (2007). Integrated neodeterministic scenarios for reliable earthquake hazard assessment, Invited lecture IASPEI Symposium SS002, Perugia, July 2007, abstract.
- Peresan, A., Panza, G.F., Gorshkov, A.I. and Aoudia, A., (2002a). Pattern recognition methodologies and deterministic evaluation of seismic hazard: a strategy to increase earthquake preparedness. Bollettino della Società Geologica Italiana, 1, 37-46.

Selected References 4

- Peresan, A., Rotwain, I., Zaliapin, I. and Panza, G.F. (2002b). Stability of intermediate-term earthquake predictions with respect to random errors in magnitude: the case of central Italy. PEPI, 130, 117-127.
- Peresan, A., Kossobokov, V., Romashkova, L. and Panza, G.F., (2005). Intermediate-term middle-range earthquake predictions in Italy: a review. Earth-Science Reviews 69 (2005) 97-132.
- Peresan A., Zuccolo E., Vaccari F. and Panza, G.F., (2007). Neo-deterministic Seismic hazard scenarios for North-Eastern Italy. Bollettino della Società Geologica Italiana. In press.
- Vaccari, F., Romanelli, F. and Panza, G.F., (2005). Detailed modelling of strong ground motion in Trieste; Modellazione dettagliata del moto sismico del suolo a Trieste. Geologia tecnica & ambientale, 2/2005, 7-40.
- ***PAGEOPH Topical Volume: Advanced Seismic Hazard Assessments; Editors:*** *G.F. Panza, K. Irikura, M. Kouteva, A. Peresan, Z. Wang, R. Saragoni, 2011*. Part I: Seismic Hazard Assessment, ISBN 978-3-0348-0039-6; Part II: Regional Seismic Hazard and Seismic Microzonation Case Studies, ISBN: 978-3-0348-0091-4, 1st Edition., 2011

105

THE END

106